On the Impact of Phase Shifting Designs on IRS-NOMA

Zhiguo Ding, *Fellow, IEEE*, Robert Schober, *Fellow, IEEE*, and H. Vincent Poor, *Life Fellow, IEEE*

***Abstract*—In this letter, the impact of two phase shifting designs, namely coherent phase shifting and random discrete phase shifting, on the performance of intelligent reflecting surface (IRS) assisted non-orthogonal multiple access (NOMA) is studied. Analytical and simulation results are provided to show that the two designs achieve different tradeoffs between reliability and complexity. To further improve the reception reliability of the random phase shifting design, a low-complexity phase selection scheme is also proposed in this letter.**

***Index Terms*—Non-orthogonal multiple access (NOMA), intelligent reflecting surface (IRS), phase shifting designs.**

I. Introduction

RECENTLY, intelligent reflecting surfaces (IRSs) have received significant attention, due to their ability to intelligently reconfigure wireless communication environments for better reception reliability at a low cost [1]–[4]. As a new energy and spectrally efficient technique, IRSs have been shown to be compatible with various advanced communication techniques, including millimeter-wave communications, unmanned aerial vehicle networks, physical layer security, and simultaneous wireless information and power transfer [5]–[7].

In this letter, we investigate the combination of IRSs and non-orthogonal multiple access (NOMA). The combination of the two techniques has been previous studied in [8]–[11] from an optimization perspective. The main contribution of this letter is to analyze the performance of IRS-NOMA, where the impact of two simple but effective phase sifting designs on IRS-NOMA is characterized. Particularly, the first considered design is coherent phase shifting, where the phase shift of each reflecting element is matched to the phases of its incoming and outgoing fading channels. The second considered design is random discrete phase shifting, which avoids the system overhead caused by acquiring channel state information (CSI) at the source, and is also motivated by the fact that coherent phase shifting might not be applicable in practice because of the finite resolution of practical phase shifters [12]. The central limit theorem (CLT) is shown to be an accurate approximation tool for analyzing the performance of random discrete phase shifting, but not for coherent phase shifting. This motivates the development of an upper bound on the outage performance, which is more accurate than the CLT-based result at high signal-to-noise ratio (SNR). In addition, a low-complexity phase selection scheme is also proposed in this letter, in order to improve the reception reliability of the random phase shifting design.

Manuscript received March 15, 2020; accepted March 26, 2020. Date of publication April 28, 2020; date of current version October 7, 2020. The work of Zhiguo Ding was supported by the U.K. Engineering and Physical Sciences Research Council under Grant EP/P009719/2. The work of H. Vincent Poor was supported by the U.S. National Science Foundation under Grant CCF-1908308. The associate editor coordinating the review of this article and approving it for publication was J. Choi. *(Corresponding author: Zhiguo Ding.)*

Zhiguo Ding is with the Department of Electrical Engineering, Princeton University, Princeton, NJ 08544 USA, and also with the School of Electrical and Electronic Engineering, University of Manchester, Manchester M13 9PL, U.K. (e-mail: zhiguo.ding@manchester.ac.uk).

Robert Schober is with the Institute for Digital Communications, Friedrich–Alexander-University Erlangen–Nürnberg, 91054 Erlangen, Germany.

H. Vincent Poor is with the Department of Electrical Engineering, Princeton University, Princeton, NJ 08544 USA.

Digital Object Identifier 10.1109/LWC.2020.2991116

II. System Model

Consider a cooperative communication scenario with one source and two users, denoted by U_1 and U_2, respectively. We assume that a direct link is not available between the source and U_1 due to severe blockage. Three cooperative communication strategies are described in the following subsections.

1) *IRS-NOMA:* IRS-NOMA ensures that the two users are simultaneously served. In particular, the source broadcasts the superimposed message, $s = c_1 s_1 + c_2 s_2$, where s_i denotes the unit-power signal for U_i, c_i denotes the power allocation coefficient, and we assume that $c_1 \geq c_2$ and $c_1^2 + c_2^2 = 1$.

The signals received by U_1 and U_2 are given by

$$y_1 = \frac{\mathbf{g}_1^H \mathbf{\Theta} \mathbf{g}_0}{\sqrt{L(d_r)L(d_{r1})}} \sqrt{P_s}(c_1 s_1 + c_2 s_2) + w_1, \quad (1)$$

and

$$y_2 = \left(\frac{h_2}{\sqrt{L(d_2)}} + \frac{\mathbf{g}_2^H \mathbf{\Theta} \mathbf{g}_0}{\sqrt{L(d_r)L(d_{r2})}} \right) \sqrt{P_s} s + w_2, \quad (2)$$

where P_s denotes the power used by the source, $\mathbf{\Theta}$ denotes the $N \times N$ diagonal phase shifting matrix with its N main diagonal elements representing the reflecting elements of the IRS, $\mathbf{g}_i$ denotes the fading vector between the IRS and U_i, $\mathbf{g}_0$ denotes the fading vector between the source and the IRS, h_2 and d_2 denote the channel gain and the distance from the source to U_2, respectively, d_r and d_{ri} denote the distances from the IRS to the source and U_i, respectively, w_i denotes the noise at U_i, $L(d)$ (in dB) $\triangleq 35.1 + 36.7 \log_{10}(d) - G_t - G_r$ denotes the effective path loss [13], G_t and G_r denote the antenna gains at the transmitter and receiver, respectively. We assume that the noise power is normalized and all channel gains are complex Gaussian distributed with zero means and unit variances, $\mathcal{CN}(0, 1)$. We also note that, because of path loss, the reflected path in (2) can be significantly weaker than the direct link. For example, for a scenario with $d_2 = d_r$, $d_{r2} = 10$ m and $G_t = G_r = 10$ dBi, U_2's reflected path is 10^4 times weaker than its direct link, which means that the reflected path can be ignored, and U_2's outage probability is similar to that in the conventional case without IRSs. Therefore, we focus only on U_1's outage probability in this letter.

U_1 treats s_2 as noise when decoding its own signal, s_1, which means that its outage probability is given by

$$\mathrm{P}_1^{\mathrm{NOMA}} = \mathrm{P}\left(\log\left(1 + \frac{P_s c_1^2 \frac{\left|\mathbf{g}_1^H \mathbf{\Theta} \mathbf{g}_0\right|^2}{L(d_r)L(d_{r1})}}{P_s c_2^2 \frac{\left|\mathbf{g}_1^H \mathbf{\Theta} \mathbf{g}_0\right|^2}{L(d_r)L(d_{r1})} + 1} \right) < R_1 \right), \quad (3)$$

where R_i denotes U_i's target data rate and P(E) denotes the probability of event E.

2) *Conventional Relaying:* The authors of [13] recently pointed out that conventional relaying can outperform IRS assisted transmission due to the excess path loss experienced by the IRS. Therefore, conventional relaying which involves two transmission phases is used as a benchmarking scheme in this letter. The first phase is further divided into two time slots. During the first time slot, the source sends s_1 to U_2, and during the second time slot, U_2 serves as a relay and forwards s_1 to U_1, if it can decode s_1. Otherwise, U_2 remains silent. During the second phase, the source serves U_2 directly. It is straightforward to show that the corresponding achievable outage probability is $\mathrm{P}_1^{\mathrm{OMA}} = (1 - e^{-L(d_2)(2^{4R_1}-1)P_1^{-1}}) + e^{-L(d_2)(2^{4R_1}-1)P_1^{-1}}(1 - e^{-L(d_{12})(2^{4R_1}-1)P_r^{-1}})$, where d_{12} denotes the distance between the two users, P_1 denotes the source's transmit power for U_1's signal, and P_r denotes the relay transmit power.

3) *IRS-OMA:* IRS assisted cooperative OMA also includes two phases. During the *i*-th phase, the source serves U_i with the help of the IRS. Therefore, the outage probability experienced by U_1 is given by

$$\mathrm{P}_1^{\mathrm{I-OMA}} = \mathrm{P}\left(\frac{1}{2}\log\left(1 + P_0\frac{\left|\mathbf{g}_1^H\mathbf{\Theta}\mathbf{g}_0\right|^2}{L(d_r)L(d_{r1})}\right) < R_1\right), \quad (4)$$

where P_0 denotes the transmit power in IRS-OMA.

III. Performance Analysis

The evaluation of the outage probabilities, $\mathrm{P}_1^{\mathrm{NOMA}}$ and $\mathrm{P}_1^{\mathrm{I-OMA}}$, depends on how the phase shifting matrix $\mathbf{\Theta}$ is designed, where two designs with different tradeoffs between performance and complexity are introduced in the following.

A. Coherent Phase Shifting

Define $\mathbf{g}_i^H\mathbf{\Theta}\mathbf{g}_0$ as follows:

$$\xi_N \triangleq \mathbf{g}_i^H\mathbf{\Theta}\mathbf{g}_0 = \sum_{n=1}^{N} e^{-j\theta_n} g_{0,n}g_{i,n}, \quad (5)$$

where $g_{i,n}$ and $g_{0,n}$ denote the n-th elements of $\mathbf{g}_i$ and $\mathbf{g}_0$, respectively, and θ_n denotes the phase shift of the n-th reflecting element of the IRS.

Assume that the phase of $g_{0,n}g_{i,n}$ can be acquired by the source. For the coherent phase shifting design, the phase shifts of the IRS are matched with the phases of the IRS fading gains, which yields the following:

$$\xi_N = \sum_{n=1}^{N} \left|g_{0,n}g_{i,n}\right|. \quad (6)$$

Despite the fact that the use of coherent phase shifting is intuitive, there is little literature on its outage performance. The main reason is that the probability density function (pdf) of ξ_N is difficult to obtain. We will provide two methods to tackle this difficulty, one based on the CLT and the other one based on an upper bound on the Bessel function.

1) CLT-Based Approximation: We note that the $|g_{0,n}g_{i,n}|$, $1 \le n \le N$, are independent and identically distributed (i.i.d.), and hence ξ_N is a sum of i.i.d. random variables, which motivates the use of the CLT.

As shown in [14], [15], the pdf of $|g_{0,n}g_{i,n}|^2$ is given by

$$f_{|g_{0,n}g_{i,n}|^2}(x) = 2K_0\left(2\sqrt{x}\right), \quad (7)$$

which can be used to find the pdf of $|g_{0,n}g_{i,n}|$ as follows:

$$f_{|g_{0,n}g_{i,n}|}(y) = 4yK_0(2y), \quad (8)$$

where $K_i(\cdot)$ denotes the i^{th}-order modified Bessel function of the second kind.

The use of the CLT requires the mean and the variance of $|g_{0,n}g_{i,n}|$, which can be obtained as follows:

$$\mu_{|g_{0,n}g_{i,n}|} = \int_0^\infty 4y^2K_0(2y)\,dy = \frac{\pi}{4}, \quad (9)$$

and

$$\sigma^2_{|g_{0,n}g_{i,n}|} = \int_0^\infty 4y^3K_0(2y)\,dy - \frac{\pi^2}{16} = 1 - \frac{\pi^2}{16}, \quad (10)$$

which follows from [16, eq. (6.561.16)]. By using the CLT, ξ_N can be approximated as the following Gaussian random variable:

$$\sqrt{N}\left(\frac{\xi_N}{N} - \mu_{|g_{0,n}g_{i,n}|}\right) \sim \mathcal{N}\left(0, \sigma^2_{|g_{0,n}g_{i,n}|}\right). \quad (11)$$

Therefore, the outage probability of IRS-NOMA can be approximated as follows:

$$\begin{aligned}\mathrm{P}_1^{\mathrm{NOMA}} &= \mathrm{P}\left(\mathbf{g}_1^H\mathbf{\Theta}\mathbf{g}_0 < \sqrt{\epsilon_1}\right)\\ &\approx \frac{1}{2} + \frac{1}{2}\phi\left(\frac{\sqrt{N}\left(\frac{\sqrt{\epsilon_1}}{N} - \mu_{|g_{0,n}g_{i,n}|}\right)}{\sqrt{2}\sigma_{|g_{0,n}g_{i,n}|}}\right), \quad (12)\end{aligned}$$

where $\epsilon_1 = \frac{L(d_r)L(d_{r1})\epsilon}{P_s(c_1^2 - \epsilon c_2^2)}$, $\epsilon = 2^{R_1} - 1$, and $\phi(x) \triangleq \frac{2}{\sqrt{\pi}}\int_0^x e^{-t^2}\,dt$. It is assumed in this letter that $c_1^2 > \epsilon c_2^2$, otherwise $\mathrm{P}_1^{\mathrm{NOMA}} = 1$. The outage probability for IRS-OMA can be obtained similarly by replacing ϵ_1 with $\epsilon_2 = \frac{L(d_r)L(d_{r1})(2^{2R_1}-1)}{P_0}$ in (12).

2) An Upper Bound: As shown in Section IV, the CLT-based approximation is not accurate in the high SNR regime, which motivates the development of a tight bound for the outage probability. To this end, we focus on IRS-NOMA. An upper bound on the outage probability is given in the following lemma.

Lemma 1: Assume that N is an even number and denote $\bar{N} = \frac{N}{2}$. The outage probability achieved by IRS-NOMA is upper bounded as follows:

$$\mathrm{P}_1^{\mathrm{NOMA}} \le \frac{2^N\pi^{\frac{N}{2}}\Gamma^N\left(\frac{3}{2}\right)}{(3\bar{N}-1)!}2^{-3\bar{N}}\gamma\left(3\bar{N}, 2\sqrt{\epsilon_1}\right), \quad (13)$$

where $\gamma(\cdot,\cdot)$ denotes the incomplete gamma function and $\Gamma(\cdot)$ denotes the gamma function.

Proof: See Appendix A. ∎

Remark: At high SNR, $\epsilon_1 \to 0$, which yields the following approximation for the upper bound shown in (13):

$$\mathrm{P}_1^{\mathrm{NOMA}} \le 2^{N-3\bar{N}}\pi^{\frac{N}{2}}\Gamma^N\left(\frac{3}{2}\right)\frac{2^{3\bar{N}}}{(3\bar{N})!}\epsilon_1^{\frac{3}{4}N} \doteq \frac{1}{P_0^{\frac{3}{4}N}}, \quad (14)$$

where $\doteq$ denotes exponential equality [17]. Eq. (14) indicates that $\frac{3}{4}N$ is an achievable diversity order. It is important to point out that the full diversity gain, N, is also achievable, as

shown in the following. By using the fact that $\xi_N \geq |g_{0,n} g_{i,n}|$, for $1 \leq n \leq N$, $\mathrm{P}_1^{\mathrm{NOMA}}$ can be upper bounded as follows:

$$\mathrm{P}_1^{\mathrm{NOMA}} \leq \left(\int_0^{\epsilon_1} f_{|g_{0,n} g_{i,n}|^2}(x)\, dx \right)^N = \left(1 - 2\epsilon_1^{\frac{1}{2}} K_1\left(2\epsilon_1^{\frac{1}{2}} \right) \right)^N \approx (-\epsilon_1 \log \epsilon_1)^N \doteq \frac{1}{P_0^N}, \quad (15)$$

which shows that the full diversity gain N is achievable. Although the upper bound in (15) is useful for the study of the diversity gain, we note that it is a bound much looser than the upper bound shown in Lemma 1, particularly for the case of large N. $\mathrm{P}_1^{\mathrm{I-OMA}}$ can be similarly bounded as $\mathrm{P}_1^{\mathrm{NOMA}}$.

B. Random Discrete Phase Shifting

The use of random discrete phase shifting can avoid the assumption of phase adjustment with perfect resolution and reduce the system overhead needed for acquiring global CSI at the source. For this considered phase shifting design, θ_n shown in (5) is discrete and randomly chosen.

Different from the coherent phase shifting case, ξ_N is a sum of complex-valued random variables, and the imaginary and real parts of $e^{-j\theta_n} g_{0,n} g_{i,n}$ are correlated, which means that the CLT is not directly applicable. In the following, we will show that ξ_N can be still approximated as a complex Gaussian random variable. We first note that, for small N, ξ_N is not complex Gaussian distributed, as can be seen from the following special case.

Proposition 1: For the special case of $N = 1$, the pdfs of the real and imaginary parts of ξ_N are same and given by

$$f_{\mathrm{Re}\{\xi_1\}}(x) = e^{-2|x|}. \quad (16)$$

Proof: See Appendix B. ∎

However, by increasing N, the Gaussian approximation becomes applicable to ξ_N, as shown in the following lemma.

Lemma 2: When $N \to \infty$, ξ_N can be approximated as a complex Gaussian random variable with zero mean and variance N, i.e.,

$$\xi_N \sim \mathcal{CN}(0, N). \quad (17)$$

Proof: See Appendix C. ∎

Therefore, the outage probabilities achieved by IRS with random phase shifting can be approximated as follows:

$$\mathrm{P}_1^{\mathrm{NOMA}} \approx 1 - e^{-\frac{\epsilon_1}{N}}, \ \& \ \mathrm{P}_1^{\mathrm{I-OMA}} \approx 1 - e^{-\frac{\epsilon_2}{N}}, \quad (18)$$

which indicates that IRS transmission with random discrete phase shifting realizes a diversity order of one.

Phase shift selection: As shown in the next section, random phase shifting cannot effectively use the available spatial degrees of freedom, although it can be implemented at low complexity. A better tradeoff between performance and complexity can be realized by carrying out phase shift selection, as described in the following. Denote by Q the number of sets of random discrete IRS phase shifts. The source sends Q pilot symbols while the IRS cycles through the Q sets of phase shifts. Then, U_1 informs the source via the IRS which set of phase shifts it prefers. The use of this simple phase selection can significantly improve the performance of IRS transmission, as shown in the next section. We also note that the effective channel gains, ξ_N, obtained with different sets of random phases are not independent, which makes it difficult to develop analytical results for the proposed phase selection scheme.

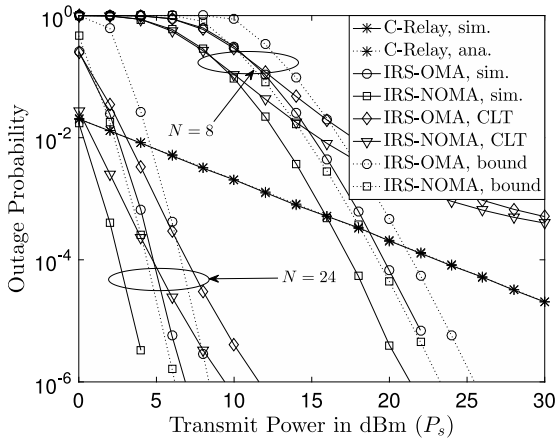

Fig. 1. IRS-OMA and IRS-NOMA with the coherent phase shifting scheme vs. conventional relaying.

IV. Numerical Studies

In this section, the performance of the three considered transmission schemes is evaluated by computer simulations. For purposes of illustration, we choose $c_1^2 = 0.8$, $c_2^2 = 0.2$, $G_t = G_r = 10$ dBi, $R_1 = 1.5$ bit per channel use (BPCU), and the noise power is -94 dBm. For a fair comparison, we use $P_1 = P_2 = P_r = P_s = P_0$, which ensures that the total energy consumed by the three schemes is the same. In addition, we use $d_2 = d_r = 10$ m and $d_{r1} = d_{12} = 15$ m, such that the distances for the IRS are the same as those for the relay in conventional relaying (i.e., U_2). Coherent phase shifting is studied first in Fig. 1. As can be observed in the figure, conventional relaying can outperform the two IRS transmission schemes, particularly in the low SNR regime. This performance loss is due to the fact that IRS transmission suffers from severe path loss, $L(d_r)L(d_{r1})$, as previously pointed out in [13]. However, by increasing the transmit power or the number of reflecting elements on the IRS, the IRS schemes eventually outperform conventional relaying, where the performance of IRS-NOMA is always better than that of IRS-OMA. The accuracy of the developed CLT approximation and the upper bound is also evaluated in the figure. As can be seen from the figure, in the low SNR regime, the CLT-based approximation is accurate, and the developed upper bound is more accurate in the high SNR regime. The inaccuracy of the CLT approximation is possibly due to the fact that the distribution of $|g_{0,n} g_{i,n}|$ shown in (8) is skewed. In addition, the CLT-based approximation (12) has an error floor, since the probability shown in (12) becomes a constant, $\frac{1}{2} - \frac{1}{2}\phi(\frac{\sqrt{N}\mu_{|g_{0,n} g_{i,n}|}}{\sqrt{2}\sigma_{|g_{0,n} g_{i,n}|}})$, for $P_s \to \infty$, which explains why the developed upper bound is more accurate at high SNR.

In Fig. 2, the impact of random discrete phase shifting on IRS transmission is investigated, where one-bit resolution phase shifting is used, i.e., each phase shift θ_n is randomly chosen from 0 and π. Recall that the motivation to use random phase shifting is that it can significantly reduce the system overhead and does not require complicated phase control mechanisms compared to coherent phase shifting. However, Fig. 2 shows that conventional relaying outperforms IRS transmission, although increasing N is helpful to reduce the performance gap. The reason for this performance loss is that random phase shifting cannot efficiently utilize the spatial degrees of freedom offered by the IRS. By implementing the proposed phase selection

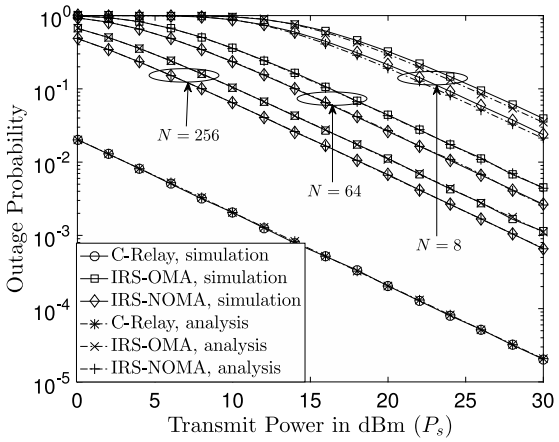

Fig. 2. Performance of random discrete phase shifting.

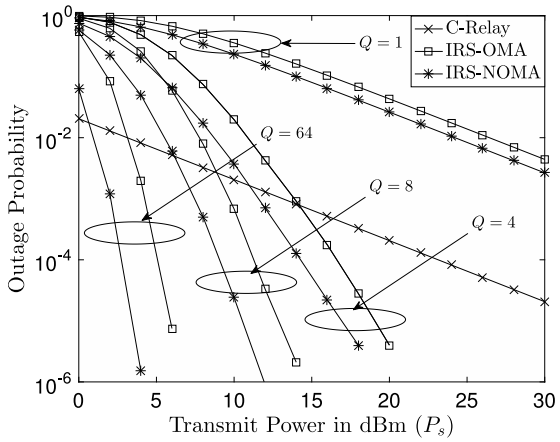

Fig. 3. Performance of phase shift selection. $N = 64$.

scheme, the performance of IRS transmission can be significantly improved. As shown in Fig. 3, with $Q = 4$, IRS-NOMA can realize a power reduction of 8 dBm at an outage probability of 10^{-4}, compared to conventional relaying, where this gain can be doubled with $Q = 8$. Figs. 2 and 3 also show that IRS-NOMA always outperforms IRS-OMA, which is consistent with Fig. 1. Furthermore, Fig. 2 demonstrates the accuracy of the approximation based on Lemma 2.

V. Conclusion

In this letter, the impact of two different phase shifting designs on the performance of IRS-NOMA has been studied. Analytical results were developed to show that the two designs achieve different tradeoffs between system performance and complexity. For coherent phase shifting, the pdf of the effective channel gain, ξ_N, was evaluated by using two types of approximations, and finding an exact expression for the pdf is an important direction for future research.

Appendix A
Proof for Lemma 1

Evaluating the outage probability achieved by IRS-OMA requires the pdf of $|g_{0,n}g_{i,n}|$, denoted by $f_{|g_{0,n}g_{i,n}|}(y_i)$, which contains the zeroth-order Bessel function. We note that an upper bound on the Bessel function was provided in [18] as follows:

$$K_0(x) \leq \frac{\sqrt{\pi}e^{-x}}{\sqrt{2x}}. \tag{19}$$

By using this upper bound on the Bessel function, the pdf of $|g_{0,n}g_{i,n}|$ shown in (8) can be upper bounded as follows:

$$f_{|g_{0,n}g_{i,n}|}(y) \leq 4y\frac{\sqrt{\pi}e^{-2y}}{\sqrt{4y}} = 2\pi^{\frac{1}{2}}y^{\frac{1}{2}}e^{-2y} \triangleq g(y). \tag{20}$$

Because of the simple expression of $g(y)$, an upper bound on the pdf of the sum, $\sum_{i=1}^{N} y_i$, can be obtained, as shown in the following. First, the Laplace transform of the upper bound $g(y)$ can be obtained as follows:

$$\mathcal{L}(g(y)) = 2\pi^{\frac{1}{2}}\int_0^{\infty} e^{-sy}y^{\frac{1}{2}}e^{-2y}dy = \frac{2\pi^{\frac{1}{2}}\Gamma\left(\frac{3}{2}\right)}{(s+2)^{\frac{3}{2}}}. \tag{21}$$

By using the fact that y_i is i.i.d., the pdf of the sum, denoted by $f_{\sum_{i=1}^{N} y_i}(y)$, can be upper bounded as follows:

$$f_{\sum_{i=1}^{N} y_i}(y) \leq \mathcal{L}^{-1}\left(\frac{2^N\pi^{\frac{N}{2}}\Gamma^N\left(\frac{3}{2}\right)}{(s+2)^{\frac{3N}{2}}}\right). \tag{22}$$

Assume that N is an even number and let $\bar{N} = \frac{N}{2}$. An upper bound on the pdf of the sum can be obtained as follows:

$$f_{\sum_{i=1}^{N} y_i}(y) \leq \frac{2^N\pi^{\frac{N}{2}}\Gamma^N\left(\frac{3}{2}\right)}{(3\bar{N}-1)!}y^{3\bar{N}-1}e^{-2y}. \tag{23}$$

Therefore, the outage probability achieved by IRS-OMA can be upper bounded as follows:

$$\mathrm{P}_1^{\mathrm{I-OMA}} \leq \int_0^{\sqrt{\epsilon_1}} \frac{2^N\pi^{\frac{N}{2}}\Gamma^N\left(\frac{3}{2}\right)}{(3\bar{N}-1)!}y^{3\bar{N}-1}e^{-2y}dy, \tag{24}$$

which can be used to obtain (13). Thus, the lemma is proved.

Appendix B
Proof for Proposition 1

Recall that $g_{0,n}$ and $g_{i,n}$ are complex Gaussian distributed with zero means and unit variances, i.e., $g_{0,n} \sim \mathcal{CN}(0,1)$ and $g_{i,n} \sim \mathcal{CN}(0,1)$. Without loss of generality, denote $g_{0,n}$ and $g_{i,n}$ by $g_{0,n} = a_n + jb_n$ and $g_{i,n} = c_n + jd_n$, respectively, where a_n, b_n, c_n, and d_n are i.i.d., and follow $\mathcal{N}(0, \frac{1}{2})$. Therefore, ξ_1 can be written as follows:

$$\begin{aligned}\xi_1 = {} & (a_nc_n - b_nd_n)\cos\theta_n - (a_nd_n + b_nc_n)\sin\theta_n \\ & + j((a_nc_n - b_nd_n)\sin\theta_n + (a_nd_n + b_nc_n)\cos\theta_n).\end{aligned} \tag{25}$$

We note that the real and imaginary parts of ξ_1 are identically distributed, and hence in the following, we focus on the real part of ξ_1 which can be further written as $\mathrm{Re}\{\xi_1\} = a_n\tilde{c}_n - b_n\tilde{d}_n$, where $\tilde{c}_n$ and $\tilde{d}_n$ are defined as follows:

$$\begin{bmatrix}\tilde{c}_n \\ \tilde{d}_n\end{bmatrix} = \begin{bmatrix}\cos\theta_n & -\sin\theta_n \\ \sin\theta_n & \cos\theta_n\end{bmatrix}\begin{bmatrix}c_n \\ d_n\end{bmatrix}. \tag{26}$$

We further note that the transformation matrix in (26) is a unitary matrix, and c_n and d_n are i.i.d. Gaussian random variables, which means that $\tilde{c}_n, \tilde{d}_n \sim \mathcal{N}(0, \frac{1}{2})$.

Therefore, the cumulative distribution function (CDF) of $\mathrm{Re}\{\xi_1\}$ is given by

$$\begin{aligned}\mathrm{P}(\mathrm{Re}\{\xi_1\} < y) &= \mathrm{P}(a_n\tilde{c}_n - b_n\tilde{d}_n < y) \\ &\overset{(a)}{=} \mathcal{E}_{\tilde{c}_n,\tilde{d}_n}\left\{\int_{-\infty}^{y}\frac{1}{\sqrt{\pi(\tilde{c}_n^2+\tilde{d}_n^2)}}e^{-\frac{x^2}{\tilde{c}_n^2+\tilde{d}_n^2}}dx\right\},\end{aligned} \tag{27}$$

where $\mathcal{E}\{\cdot\}$ denotes the expectation, step (a) follows from the fact that $a_n\tilde{c}_n - b_n\tilde{d}_n$ is a sum of two i.i.d. Gaussian variables,

a_n and b_n, by treating $\tilde{c}_n$ and $-\tilde{d}_n$ as the weighting constants. By using the fact that $z \triangleq \tilde{c}_n^2 + \tilde{d}_n^2$ is exponentially distributed, the CDF of $\mathrm{Re}\{\xi_1\}$ is given by

$$\mathrm{P}(\mathrm{Re}\{\xi_1\} < y) = \int_0^{\infty} \int_{-\infty}^{y} \frac{1}{\sqrt{\pi z}} e^{-\frac{x^2}{z}} dx e^{-z} dz. \quad (28)$$

The CDF of $\mathrm{Re}\{\xi_1\}$ can be simplified as follows:

$$\begin{aligned} \mathrm{P}(\mathrm{Re}\{\xi_1\} < y) &= \int_{-\infty}^{y} \frac{1}{\sqrt{\pi}} \int_0^{\infty} z^{-\frac{1}{2}} e^{-\frac{x^2}{z} - z} dz dx \\ &\overset{(b)}{=} \int_{-\infty}^{y} e^{-2|x|} dx, \end{aligned} \quad (29)$$

where step (b) follows from [16, eq. (3.471.15)]. By finding the derivative of the CDF, the pdf in the proposition can be obtained and the proof is complete.

Appendix C
Proof for Lemma 2

The lemma can be proved in two steps as shown in the following two subsections.

A. $\mathrm{Re}\{\xi_N\}, \mathrm{Im}\{\xi_N\} \sim \mathcal{N}(0, \frac{N}{2})$ for $N \to \infty$

Since $\mathrm{Re}\{\xi_N\}$ and $\mathrm{Im}\{\xi_N\}$ are identically distributed, we will focus on $\mathrm{Re}\{\xi_N\}$, without loss of generality. Recall that $\mathrm{Re}\{\xi_N\} = \sum_{n=1}^{N} \mathrm{Re}\{e^{-j\theta_n} g_{0,n} g_{i,n}\}$.

Without directly using the CLT, the approximation for the pdf of $\mathrm{Re}\{\xi_N\}$ can be straightforwardly obtained as follows. By applying Proposition 1, the characteristic function of the pdf of $\mathrm{Re}\{e^{-j\theta_n} g_{0,n} g_{i,n}\}$ can be obtained as follows:

$$\psi_{\mathrm{Re}\{e^{-j\theta_n} g_{0,n} g_{i,n}\}}(t) = \int_{-\infty}^{\infty} e^{itx} f_{\xi_1}(x) dx = \frac{4}{4 + t^2}. \quad (30)$$

By using the fact that $\mathrm{Re}\{e^{-j\theta_n} g_{0,n} g_{i,n}\}$ is independent from $\mathrm{Re}\{e^{-j\theta_m} g_{0,m} g_{i,m}\}$ for $n \neq m$, the characteristic function of the pdf of $\mathrm{Re}\{\xi_N\}$ can be obtained as follows:

$$\psi_{\mathrm{Re}\{\xi_N\}}(t) = \frac{4^N}{(4 + t^2)^N} \underset{N \to \infty}{\to} e^{-\frac{Nt^2}{4}}, \quad (31)$$

where the approximation follows by applying the limit of the exponential function. Therefore, $\mathrm{Re}\{\xi_N\}$ can be approximated as a Gaussian random variable since $e^{-\frac{Nt^2}{4}}$ is the characteristic function of a Gaussian random variable.

B. $\mathrm{Re}\{\xi_N\}$ and $\mathrm{Im}\{\xi_N\}$ are Independent for $N \to \infty$

We have proved that $\mathrm{Re}\{\xi_N\}, \mathrm{Im}\{\xi_N\} \sim \mathcal{N}(0, \frac{N}{2})$, for $N \to \infty$. Therefore, the independence of the two random variables can be proved by showing them to be jointly Gaussian distributed and also uncorrelated.

In order to show that $\mathrm{Re}\{\xi_N\}$ and $\mathrm{Im}\{\xi_N\}$ are jointly Gaussian distributed, we first build an arbitrary linear combination of $\mathrm{Re}\{\xi_N\}$ and $\mathrm{Im}\{\xi_N\}$ with β_1 and β_2 as follows:

$$\begin{aligned} &\beta_1 \mathrm{Re}\{\xi_N\} + \beta_2 \mathrm{Im}\{\xi_N\} \\ &\quad = \sum_{n=1}^{N} a_n(\beta_1 \tilde{c}_n + \beta_2 \tilde{d}_n) - b_n(\beta_1 \tilde{d}_n - \beta_2 \tilde{c}_n). \end{aligned} \quad (32)$$

Note that $(\beta_1 \tilde{c}_n + \beta_2 \tilde{d}_n)$ and $(\beta_1 \tilde{d}_n - \beta_2 \tilde{c}_n)$ are independent and identically Gaussian distributed since they are constructed from $\tilde{c}_n$ and $\tilde{d}_n$ with two orthogonal coefficient vectors $[\beta_1 \quad \beta_2]^T$ and $[-\beta_2 \quad \beta_1]^T$. By following the steps in the previous subsection, it is straightforward to show that the linear combination is also Gaussian distributed, which means that $\mathrm{Re}\{\xi_N\}$ and $\mathrm{Im}\{\xi_N\}$ are jointly Gaussian distributed.

The correlation between $\mathrm{Re}\{\xi_N\}$ and $\mathrm{Im}\{\xi_N\}$ is given by

$$\begin{aligned} &\mathcal{E}\Big\{\mathrm{Re}\{\mathbf{g}_i^H \mathbf{\Theta}_p \mathbf{g}_0\} \mathrm{Im}\{\mathbf{g}_i^H \mathbf{\Theta}_p \mathbf{g}_0\}\Big\} \\ &\quad = \mathcal{E}\left\{\left(\sum_{n=1}^{N} a_n \tilde{c}_n - b_n \tilde{d}_n\right)\left(\sum_{n=1}^{N} a_n \tilde{d}_n + b_n \tilde{c}_n\right)\right\} = 0, \end{aligned} \quad (33)$$

which follows from the fact that a_n, b_n, $\tilde{c}_n$ and $\tilde{d}_n$ are i.i.d. with zero mean. Therefore, the independence of $\mathrm{Re}\{\xi_N\}$ and $\mathrm{Im}\{\xi_N\}$ is proved.

References

[1] Q. Wu and R. Zhang, "Intelligent reflecting surface enhanced wireless network via joint active and passive beamforming," *IEEE Trans. Wireless Commun.*, vol. 18, no. 11, pp. 5394–5409, Nov. 2019.

[2] M. D. Renzo *et al.*, "Smart radio environments empowered by AI reconfigurable meta-surfaces: An idea whose time has come," *EURASIP J. Wireless Commun. Netw.*, vol. 129, pp. 1–20, May 2019.

[3] Q. Wu and R. Zhang, "Towards smart and reconfigurable environment: Intelligent reflecting surface aided wireless network," *IEEE Commun. Mag.*, vol. 58, no. 1, pp. 106–112, Jan. 2020.

[4] V. Jamali, A. M. Tulino, G. Fischer, R. Müller, and R. Schober, "Intelligent reflecting and transmitting surface aided millimeter wave massive MIMO," 2019. [Online]. Available: arXiv:1902.07670.

[5] Q. Zhang, W. Saad, and M. Bennis, "Reflections in the sky: Millimeter wave communication with UAV-carried intelligent reflectors," in *Proc. IEEE Global Commun. Conf. (GLOBECOM)*, Waikoloa, HI, USA, Dec. 2019, pp. 1–6.

[6] B. Lyu, D. T. Hoang, S. Gong, D. Niyato, and D. I. Kim, "IRS-based wireless jamming attacks: When jammers can attack without power," 2020. [Online]. Available: arXiv:2001.01887.

[7] C. Pan *et al.*, "Intelligent reflecting surface aided MIMO broadcasting for simultaneous wireless information and power transfer," 2020. [Online]. Available: arXiv:1908.04863.

[8] B. Zheng, Q. Wu, and R. Zhang, "Intelligent reflecting surface-assisted multiple access with user pairing: NOMA or OMA?" *IEEE Commun. Lett.*, vol. 24, no. 4, pp. 753–757, Apr. 2020.

[9] M. Fu, Y. Zhou, and Y. Shi, "Intelligent reflecting surface for downlink non-orthogonal multiple access networks," 2019 . [Online]. Available: arXiv:1906.09434.

[10] G. Yang, X. Xu, and Y.-C. Liang, "Intelligent reflecting surface assisted non-orthogonal multiple access," 2019 . [Online]. Available: arXiv:1907.03133.

[11] J. Zuo, Y. Liu, Z. Qin, and N. Al-Dhahir, "Resource allocation in intelligent reflecting surface assisted NOMA systems," 2020. [Online]. Available: arXiv:2002.01765.

[12] Q. Wu and R. Zhang, "Beamforming optimization for intelligent reflecting surface with discrete phase shifts," in *Proc. Int. Conf. Acoust. Speech Signal Process. (ICASSP)*, Brighton, U.K., May 2019, pp. 7830–7833.

[13] E. Björnson, O. Özdogan, and E. G. Larsson, "Intelligent reflecting surface vs. decode-and-forward: How large surfaces are needed to beat relaying?" 2019. [Online]. Available: arXiv:1906.03949.

[14] Z. Ding and H. V. Poor, "A simple design of IRS-NOMA transmission," *IEEE Commun. Lett.*, vol. 24, no. 5, pp. 1119–1123, May 2020.

[15] N. C. Sagias, "On the ASEP of decode-and-forward dual-hop networks with pilot-symbol assisted M-PSK," *IEEE Trans. Commun.*, vol. 62, no. 2, pp. 510–521, Feb. 2014.

[16] I. S. Gradshteyn and I. M. Ryzhik, *Table of Integrals, Series and Products*, 6th ed. New York, NY, USA: Academic, 2000.

[17] L. Zheng and D. N. C. Tse, "Diversity and multiplexing: A fundamental tradeoff in multiple antenna channels," *IEEE Trans. Inf. Theory*, vol. 49, no. 5, pp. 1073–1096, May 2003.

[18] Z.-H. Yang and Y.-M. Chu, "On approximating the modified bessel function of the second kind," *J. Inequal. Appl.*, vol. 41, pp. 1–8, Dec. 2017.